Talanta 129 (2014) 219–226

Contents lists available at ScienceDirect

Talanta

journal homepage: www.elsevier.com/locate/talanta

Ultrasensitive electrochemiluminescent detection of cardiac troponin I based on a self-enhanced Ru(II) complex

Ying Zhou, Ying Zhuo, Ni Liao, Yaqin Chai*, Ruo Yuan*

Key Laboratory of Luminescent and Real-Time Analytical Chemistry (Southwest University), Ministry of Education, College of Chemistry and Chemical Engineering, Southwest University, Chongqing 400715, PR China

ARTICLE INFO

Article history:
Received 9 February 2014
Received in revised form
3 April 2014
Accepted 5 April 2014
Available online 14 May 2014

Keywords:
Self-enhanced
Reagentless
Electrochemiluminescence
Immunosensor
$Ru(dcbpy)_3^{2+}$
L-Cysteine
cTnI

ABSTRACT

To promote the luminous efficiency of luminophore, traditional electrochemiluminescence (ECL) immunoassay usually adopts the adding of coreactant into testing solution. However, many adverse micro-environmental factors in the solution are a limiting factor in ECL analytical techniques and received extensive attention. In our work, a self-enhanced ECL luminophore was synthesized by combining the coreactant (L-cysteine) and the luminophor (tris (4,4′-dicarboxylicacid-2,2′-bipyridyl) ruthenium(II) dichloride ($Ru(dcbpy)_3^{2+}$)) to form one Ru(II) complex and was applied to fabricate a reagentless immunosensor for the detection of cardiac troponin I (cTnI) for the first time. Herein gold nanorods (AuNRs), due to their high specific surface area and good electrocatalytic ability, were used as carriers for the immobilization of Ru(II) complex and cTnI antibody to obtain the Ab_2 bioconjugates as signal labels. The application of the self-enhanced Ru(II) complex not only avoided the addition of any coreactant into testing solution for simplifying the operation, but also achieved the intramolecular reaction for improving the ECL signal due to shorter electron transfer path and less energy loss. In view of these advantages, the proposed immunosensor achieved a wide linear range from 0.25 pg/mL to 0.1 ng/mL with an impressive detection limit of 0.083 pg/mL for cTnI ($S/N=3$).

1. Introduction

Recent years, acute myocardial infarction (AMI) has been listed as the leading cause of morbidity and mortality among cardiovascular diseases [1]. It is reported cardiac troponin I (cTnI) has been recognized as the gold standard cardiac biomarkers in the detection of AMI, because of its superior cardiac specificity and selectivity [2,3]. Therefore, highly efficient and reliable analytical techniques are necessary for measuring cTnI present at ultralow levels during early stages of disease progress. Up to date, the detection of cTnI mainly relied on sandwich-type immunoassay based on labeling technology with various inspection methods such as enzyme-linked immunoassay (ELISA) [4], optomagnetic biosensor [5], electrochemical immunoassay [6]. However, improvements are still required, as these methods remain some defects including cumbersome, time-consuming, and harmful to the environment. Electrochemiluminescence (ECL) immunosensors are of great interest because of their high sensitivity, low back ground and wide dynamic range.

One of the most extensively studied ECL luminophore is Ruthenium(II) tris(2,2′-bipyridyl) ($Ru(bpy)_3^{2+}$) or its derivatives, for the reason that $Ru(bpy)_3^{2+}$ has high quantum yields and long excited state lifetimes as well as strong luminescence [7]. Currently, to improve the ECL intensity of $Ru(bpy)_3^{2+}$, a variety of research has been focused on exploring effective co-reactants, such as peroxydisulfate [8], oxalat [9], or tripropylamine (TPA) [10]. However, many micro-environmental factors in testing solution, such as viscosity, temperature, surfactant, ion strength and pH would affect the $Ru(bpy)_3^{2+}$ ECL in solution phase [11]. To resolve these problems, the reagentless ECL sensor has been constructed by immobilizing the coreactant and the luminophore onto an electrode surface. This kind of reagentless ECL sensor can avoid external addition of reagents in analytical procedure and is a comfortable way to overcome the limitation of reagent consumed [12]. In our previous work, we also have constructed a reagentless ECL immunosensor by immobilizing the coreactant of poly-L-lysine to enhance the ECL of $Ru(bpy)_3^{2+}$ for signal amplification [13]. Although the luminous intensity of the $Ru(bpy)_3^{2+}$ is indeed enhanced, it suffers from the problems of operational complexity. Recently Swanick et al. have designed self-enhanced electrochemiluminescence of an Iridium(III) complex, which leaded to an avenue for greatly simplifying ECL detection protocols with integrated co-reactant and luminophore in a single molecule, and

* Corresponding authors. Tel.: +86 23 68252277; fax: +86 23 68253172.
E-mail addresses: yqchai@swu.edu.cn (Y. Chai), yuanruo@swu.edu.cn (R. Yuan).

http://dx.doi.org/10.1016/j.talanta.2014.04.012
0039-9140/

drastically enhancing detection sensitivity [14], but never was applied in the sensor technologies.

Several reports have pointed out many kinds of amine compounds that could act as the co-reactant to significantly enhance the ECL of $Ru(bpy)_3^{2+}$ [15]. The linear L-cysteine (L-Cys) has a backbone of two methylene followed by one amino group and one carboxy group. This gives L-Cys the attribute of serving as an proper co-reactant and linking reagent of $Ru(dcbpy)_3^{2+}$. In our work, we synthesized the self-enhanced ECL of a novel Ru(II) complex by connecting the co-reactant of L-Cys to luminophor of tris (4,4′-dicarboxylicacid-2,2′-bipyridyl) ruthenium(II) dichloride ($Ru(dcbpy)_3^{2+}$). It was found the ECL efficiency is significantly enhanced, since the intramolecular ECL reaction could be more efficient as compared with the intermolecular reaction due to the shorter electron transfer path and less energy loss.

With the advent of nanotechnology, gold nanosystems have received widespread interest in their use in biotechnological systems for diagnostic application and biological imaging owing to their unique optical properties, bioconjugation and potential non-cytotoxicity [16]. Gold nanorods (AuNRs), which are elongated nanoparticles, can provide several advantages over spherical gold nanoparticles for localized surface plasmon resonance (LSPR) sensing because of their distinct optical properties [17] and larger specific surface area [18]. These unique properties have been widely applied in the field of chemical and biochemical sensing.

Inspired by those perspectives, we presented a reagentless ECL immunosensor based on a novel Ru(II) complex as ECL labels in this work. The sensing interface was achieved by assembling cTnI antibody (anti-cTnI) on the gold nanodendrites (GNDs) modified electrode. A sandwich immunoassay format was employed to detect cTnI with the bionanorods as tracer, which were prepared based on the coimmobilization of L-Cys@$Ru(dcbpy)_3^{2+}$ molecular compounds and anti-cTnI (Ab_2) on AuNRs via Au–N or Au–S bond (Ab_2/AuNRs/L-Cys@$Ru(dcbpy)_3^{2+}$). This strategy avoided the addition of the co-reactant in testing solution and significantly simplified the immunoassay procedure, shortened the analytical time, drastically enhanced the ECL of $Ru(dcbpy)_3^{2+}$ and thus provided a new promising platform for clinical immunoassay.

2. Experimental

2.1. Reagent

Tris (4,4′-dicarboxylicacid-2,2′-bipyridyl) ruthenium(II) dichloride ($Ru(dcbpy)_3^{2+}$) was purchased from Suna Tech Inc (Shangdong, China). L-cysteine, L-ascorbic acid (AA), cetyltrimethylammonium bromide (CTAB), $AgNO_3$, $NaBH_4$ were obtained from Chengdu kelong chemical Industry (Chengdu, China). Gold chloride ($HAuCl_4 \cdot 4H_2O$) and BSA (96–99%) were received from Shanghai fine chemical materials institute (Shanghai, China). cTnI from human myocardium muscle, murine monoclonal antibody against cTnI (anti-cTnI) were obtained from Shanghai huayi Industry (Purity greater than 95%) (Shanghai, China). Phosphate buffer solutions (PBS) with pH 7.4 was prepared by mixing standard stock solutions of 0.1 M K_2HPO_4, 0.1 M NaH_2PO_4, and 0.1 M KCl and adjusting the pH with 0.1 M HCl or NaOH, then diluting with double distilled water. All chemicals were of analytical grade and used without further purification. All solutions were prepared with double distilled water and stored in the refrigerator (4 °C).

2.2. Apparatus

The ECL emission was monitored by a model MPI-A electrochemiluminescence analyzer (Xi'An Remax Electronic Science &Technology Co. Ltd., Xi An, China). Cyclic voltammetric (CV) measurements were carried out with a CHI 610A electrochemistry workstation (Shanghai CH Instruments, China). A three-electrode electrochemical cell was composed of a modified glass carbon electrode (GCE, Φ=4 mm) as the working electrode, a platinum wire as the auxiliary electrode, and a saturated calomel electrode (SCE) as the reference electrode. The morphologies of different nanomaterials were characterized by transmission electron microscopy (TEM) (H600, Hitachi, Japan) or scanning electronmicroscopy (SEM, S-4800, Hitachi, Tokyo, Japan) at an acceleration voltage of 20 kV. The UV–vis absorption spectra were recorded on a UV-2550 spectrophotometer (Shimadzu, Japan).

2.3. Preparation of AuNRs

The gold nanorods (AuNRs) were prepared via the seeded-growth mechanism as previously described with slight modifications [19]. Briefly, the seed solution was prepared by mixing 5 mL of CTAB (0.2 M) and 0.5 mL of $HAuCl_4$ (5 mM) in a vial. Then, 0.6 mL of freshly prepared 10 mM ice-cold $NaBH_4$ was quickly added. The color of the solution changed from dark yellow to brownish yellow under vigorous stirring. After 2 h, this seed solution was used for the synthesis of AuNRs.

For the synthesis of AuNRs, 40 mL of 0.2 M CTAB solution mixed with 5 mL of 10 mM $HAuCl_4$ was added to 0.25 mL of 10 mM silver nitrate aqueous solution. After gentle stirring of the solution, 0.27 mL AA (100 mM) was added to this system. 0.42 mL of the seed solution was added to the growth solution to initiate the growth of AuNRs, and then the solution was kept constant at 30 °C for 24 h. Finally, the prepared AuNRs were centrifuged for 25 min at 8000 rpm (RCF: 4448g) at least three times and dispersed in 4 mL double distilled water. Scheme 1 (A) showed the production process of AuNRs.

2.4. Preparation of self-enhanced L-Cys@$Ru(dcbpy)_3^{2+}$ molecular compounds

The overall process involved in fabricating the L-Cys@$Ru(dcbpy)_3^{2+}$ compounds was shown schematically in Fig. 1. Briefly, 97 mg L-Cys was dispersed in 4 mL acetic acid (1%) to obtain a homogeneous suspension by continuous ultrasonication. Meanwhile, 4.5 mg $Ru(dcbpy)_3^{2+}$ was dissolved in 1 mL PBS (pH 7.4) containing 400 mg EDC and 100 mg NHS with vigorous agitation for 8 h at room temperature, to active the carboxyl of $Ru(dcbpy)_3^{2+}$. Then 1 mL of 20 mM L-Cys was add into the solution and stirring for 12 h was needed, to generate the peptid bond between the NH_2 groups of L-cysteine and the COOH groups of $Ru(dcbpy)_3^{2+}$. At last, the unreacted L-Cys and $Ru(dcbpy)_3^{2+}$ were purified by dialysis (with a molecular weight cutoff of 8500) in distilled water for one day, the novel Ru(II) derivative (L-Cys@$Ru(dcbpy)_3^{2+}$) was obtained.

2.5. Preparation of Ab_2/AuNRs/L-Cys@$Ru(dcbpy)_3^{2+}$ probe (Ab_2 bioconjugates)

1 mL of the L-Cys@$Ru(dcbpy)_3^{2+}$ molecular compounds and 100 μL anti-cTnI solutions were added simultaneously into 1 mL prepared AuNRs and stirred at 4 °C for 8 h via Au–N or Au–S linking between AuNRs, anti-cTnI and Ru(II) derivative. Subsequently 200 μL bovine serum albumin (BSA, w/w, 1%) was implemented to block the unmodified portion of the AuNRs surface with the reaction time of 40 min. The final solution was centrifuged for 15 min at 8000 rpm (RCF: 4448g), the upper solution was removed and the lower products washed three times with doubly distilled water. The collected lower sediment was dispersed in 1.0 mL PBS solution (pH 7.4) to obtain Ab_2/AuNRs/L-Cys@$Ru(dcbpy)_3^{2+}$ probe

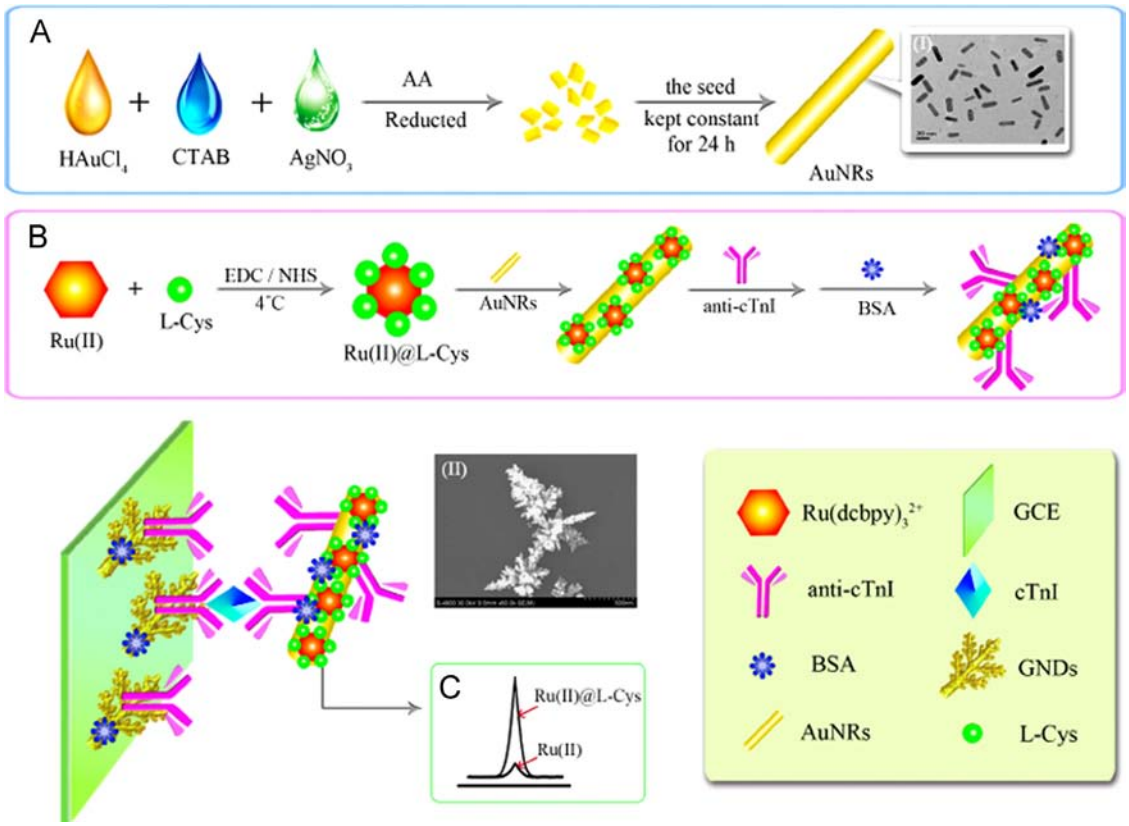

Scheme 1. The schematic diagrams of the immunosensor and signal amplification mechanism. The insert of (A) shown the diagram of preparation of AuNRs, (B) revealed the stepwise of Ab_2/AuNRs/L-Cys@Ru(dcbpy)$_3^{2+}$ probe (Ab_2 bioconjugates) fabrication, (C) shown the comparative ECL signals with self-enhanced L-Cys@Ru(II) compounds and with Ru(II) alone, then (I) and (II) displayed the TEM image of AuNRs and SEM image of the GNDs, respectively.

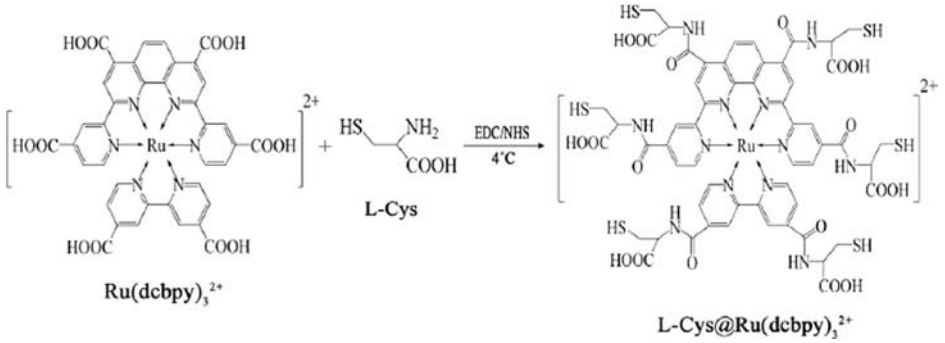

Fig. 1. A schematic diagram of the procedure used to prepare L-Cys@Ru(dcbpy)$_3^{2+}$ molecular compounds.

(Ab_2 bioconjugates). Scheme 1 (B) showed the diagram of preparation of Ab_2 bioconjugates.

2.6. Measurement procedure

The measurement was based on a sandwich immunoassay method. Before measurement, the immunosensor was incubated with different cTnI standard solutions at 37 °C for 30 min. Next, the modified electrode was incubated in Ab_2 bioconjugates for 30 min at 37 °C. Finally, the resultant immunosensor was investigated with a MPI-A electrochemiluminescence analyzer in 3 mL 0.1 M PBS (pH 7.4) at room temperature. The voltage of the photomultiplier tube (PMT) was set at 800 V and the applied potential was 0.2–1.25 V (vs. Ag/AgCl) with a scan rate of 100 mV/s in the process of detection. With the increasing cTnI antigen concentration, the amount of Ab_2/AuNRs/L-Cys@Ru(dcbpy)$_3^{2+}$ increased, which implied that the ECL signals of Ru(dcbpy)$_3^{2+}$ enhanced. Therefore, the changes of ECL intensity directly reflected the concentration changes of cTnI.

2.7. Fabrication of the electrochemiluminescence immunosensor

To obtain a mirror like surface, the GCE was first polished, respectively with 0.3, 0.05 mm alumina powder, followed by washing thoroughly with distilled water and successively sonicating in ethanol, distilled water, respectively. Before modification, the GCE was dried with nitrogen at room temperature.

After that, the GCE was immersed in 2.5 mM $HAuCl_4$ containing 0.5 M H_2SO_4 and 150 mM ethylenediamine aqueous solution for electrochemical deposition under constant potential of 0.0 V for 600 s to construct the gold nanodendrites layer (GNDs) on the electrode surface [20]. Then 15 μL of anti-cTnI (Ab_1) was dropped

onto the surface of the GNDs with 8 h incubation at 4 °C. The immunosensor was washed with double distilled water to remove the physical adsorbed Ab_1 and then 15 μL of 5% BSA solutions was placed onto the electrode for 30 min at room temperature to block the non-specific binding sites, followed by washing with double distilled water. Ultimately, the obtained immuneosensor was stored at 4 °C when not in use. The process for the fabrication of the immunosensor was shown in Scheme 1.

3. Results and discussion

3.1. Characteristics of the different nanomaterials

The size and morphologies of the synthesized nanocomposites were characterized by Transmission electronmicroscopy (TEM). The TEM of the morphology of AuNRs was shown in Fig. 2a. AuNRs exhibits a typical tubulous structure and highly dispersed. The size of the nanorod was mostly 30 nm in length and 9 nm in diameter, and then the aspectratio was about 3.3. To examine the uniformity of AuNRs, the UV absorption spectroscopy could be used for the characterization of whole dispersion. The UV–vis spectrum of the as-prepared AuNRs exhibited two distinct plasmon absorption bands centered at 476 and 727 nm (Fig. 2b), which were assigned to the transverse and longitudinal plasmon resonance absorption (PRA) of the AuNRs, indicated that AuNRs were prepared successfully [21]. Fig. 2c showed the SEM images of the GNDs straightforwardly electrodeposited on the GCE, which demonstrated that the GNDs exhibited well-defined dendritic structures, the insert of Fig. 2c showed a partially enlarged SEM image of the nanocomposites.

3.2. The stability of the L-Cys@Ru(II) compounds

To examine the stability of L-Cys@Ru(II) complex, the UV absorption spectroscopy was utilized. The $Ru(dcbpy)_3^{2+}$ exhibited two distinct plasmon absorption bands centered at 299 nm and 465 nm (Fig. 3). The absorption spectrum of the L-Cys@Ru(II) compounds red-shifted to 335 nm and 510 nm, due to the generation of peptid bond between the NH_2 groups of L-cysteine and the COOH groups of $Ru(dcbpy)_3^{2+}$ [22]. The UV–vis spectrum of carboxyl group in the L-cys exhibited one distinct plasmon absorption bands centered at 212 nm [23], however the L-Cys@Ru (II) complex did not have the absorption band in around 200 nm, which could prove the conjugation of carboxyl group. Those changes proved that the L-Cys@Ru(II) complex was successfully prepared.

3.3. Possible luminescence mechanism of L-Cys@Ru(II) compounds

Fig. 4 shown ECL (Fig. 4A, red line) and electrochemical responses (Fig. 4A, green line) obtained for Ru(II) compounds modified GCE in air-saturated PBS (pH 7.4). First, the ECL signs were not present when the potential was scanned anodically from

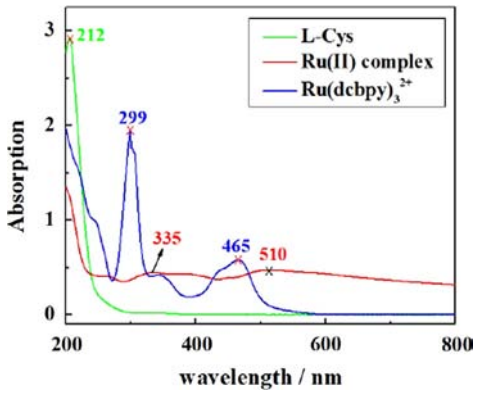

Fig. 3. UV–vis absorption spectrum of L-Cys (green line), L-Cys@Ru(II) complex (red line), and Ru(II) (blue line). (For interpretation of the references to color in this figure legend, the reader is referred to the web version of this article.)

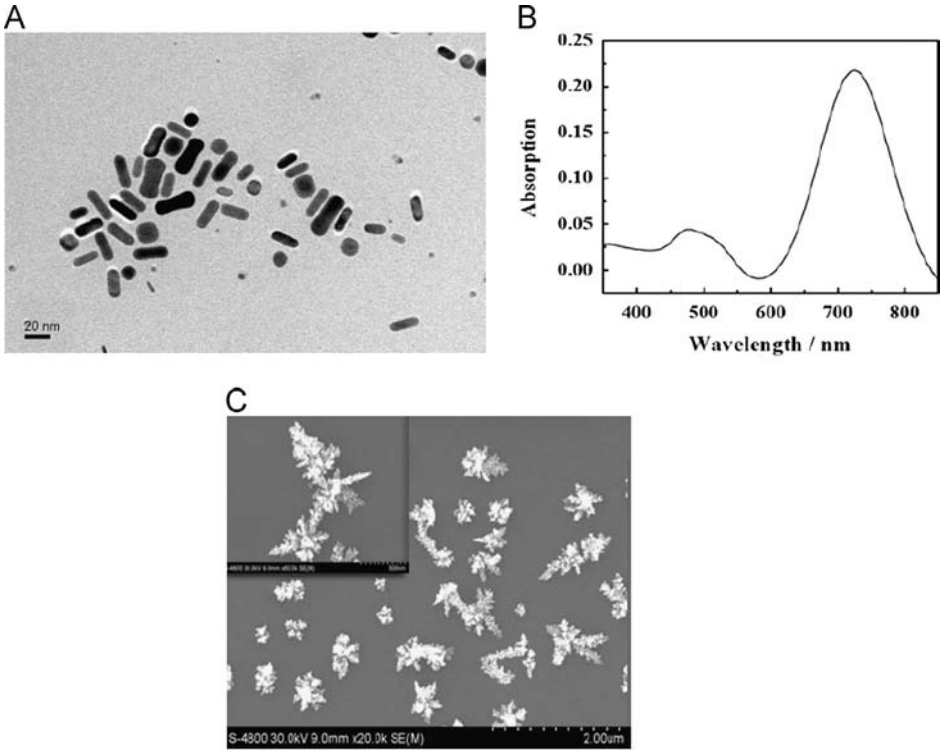

Fig. 2. (A) A TEM micrograph of AuNRs. (B) Absorption spectra of the colloidal AuNRs. (C) Showed a partially enlarged SEM image of the GNDs.

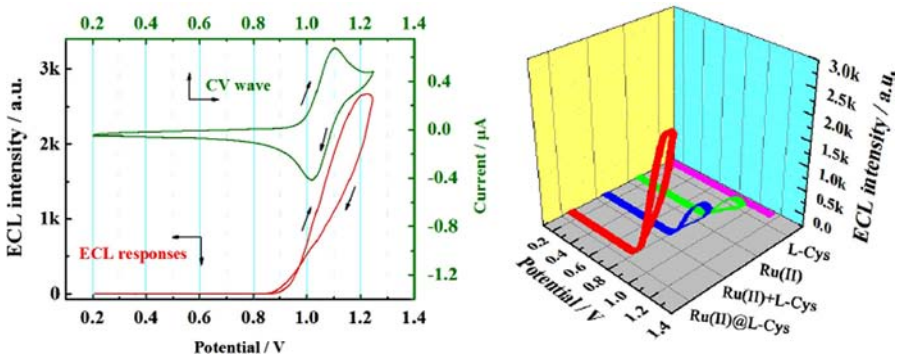

Fig. 4. (A) Cyclic voltammograms (green line) and its corresponding ECL curves (red line) of L-Cys@Ru(II) compounds modified GCE in air-saturated PBS (pH 7.4) with the potential scan of +0.2 and +1.25 V. (B) ECL curves of L-Cys@Ru(II)/GCE (red) in PBS (pH 7.4); $Ru(dcbpy)_3^{2+}$/GCE with (blue) and without (green) PEI in PBS (pH 7.4). The pink curve shows the bare GCE in the PBS containing PEI. Scan rate: 100 mV/s. (For interpretation of the references to color in this figure legend, the reader is referred to the web version of this article.)

+0.2 V to +1.0 V. Until the potential reached higher than 1.0 V, where L-Cys@Ru(II) compounds could be oxidized to L-Cys@Ru(III) compounds, a significant ECL emission was observed (with the peak intensity of 2633 a.u., Fig. 4B, red curve), indicating that the ECL was from L-Cys@Ru(II)* compounds light emission. Compared with the ECL of L-Cys@Ru(II), the $Ru(dcbpy)_3^{2+}$ modified GCE shows less ECL peak intensity (337 a.u.) when it scaned in air-saturated PBS (pH 7.4) containing L-Cys as a coreactant (Fig. 4B, blue curve). The green curve in Fig. 4B displays the ECL of $Ru(dcbpy)_3^{2+}$ modified GCE in air-saturated PBS without L-Cys as a coreactant. Only peak intensity of 132 a.u. was obtained, which could demonstrate L-Cys would enhance the ECL of $Ru(dcbpy)_3^{2+}$. Besides, no ECL peak can be observed on the bare GCE in the PBS containing L-Cys (pink curve, Fig. 4B), due to the lack of luminophor in the system. It can be found the maximum intensity and the lowest luminous potential was obtained by the self-enhanced L-Cys@Ru(II) compounds.

We supposed the ECL mechanism of the self-enhanced L-Cys@Ru(II) system based on the prevailing amine oxidation mechanism [24], as the following equations

$$L-Csy-Ru(II)2e^- \rightarrow L-Csy^{\cdot+}-Ru(III) \quad (1)$$

$$L-Csy^{\cdot+}-Ru(III) \rightarrow L-Csy^{\cdot}-Ru(III)+H^+ \quad (2)$$

$$\text{L-Cys}^{\cdot}\text{- Ru(III)} \longrightarrow \text{L-Cys- Ru(II)}^{*} \quad (3)$$

$$L-Csy-Ru(II)^* \rightarrow L-Csy-Ru(II)+hv \quad (4)$$

3.4. The electrochemical characterization of the proposed immunosensor

To characterize the fabrication process of ECL immunosensor, the cyclic voltammetric (CV) was used as an effective method to confirm the change of the sensing interface in the presence of a $K_3[Fe(CN)_6]/K_4[Fe(CN)_6]$ (1:1) mixture as redox marker. As shown in Fig. 5, when the GNDs was electrodeposited on the electrode surface, the redox peak currents were significantly higher (curve b) than that of a bare GCE (curve *a*), which was attributed to the GNDs could promote the electron transfer. Then, the electrode was modified with anti-cTnI, the peak currents were decreased (curve *c*). The reason may be that the antibody biomacromolecules acted as a nonconductor obstructing the electron transfer toward electrode surface. After the resultant electrode was blocked with BSA

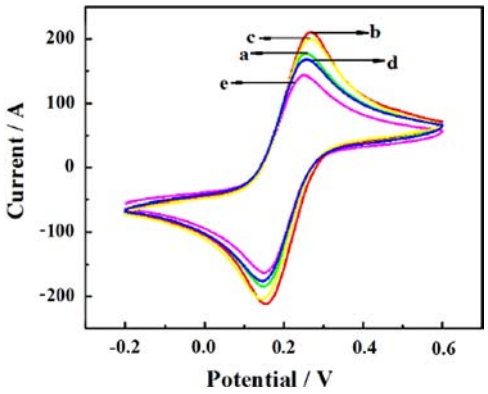

Fig. 5. CVs of different modified electrodes at pH 7.4 PBS containing 5.0 mM $K_3[Fe(CN)_6]/K_4[Fe(CN)_6]$ (1:1) as redox probe: (a) bare GCE, (b) GNDs/GCE, (c) anti-cTnI/GNDs/GCE, (d) BSA/anti-cTnI/GNDs/GCE, (e) cTnI/BSA/anti-cTnI/GNDs/GCE. Scanning of CVs was from −0.2 to 0.6 V with a rate of 100 mV/s and all potentials are given against SCE.

(curve *d*) and incubated with cTnI antigen (curve *e*), the CV responses declined in succession for the hindrance of BSA.

3.5. Optimization of incubation time for Ab_2 bioconjugates

The incubation time of Ab_2 is the important factor to form a compact and stable sandwich-type immunosensor. Ab_2 bioconjugates (Ab_2/AuNRs/L-Cys@$Ru(dcbpy)_3^{2+}$) is a complex mixture, containing chemiluminescence reagent and co-reactant. So the specificity binding of antigen and antibody is important to the stability of ECL intensity and the detection of antigen. As shown in Fig. 6, with increasing incubation time, the ECL intensity increased gradually, and then it began to stabilize after 60 min. The experiment results showed that in 70 min it could form a compact and stable immuno-complex, and enhance the ECL signal most effectively. Thus, 70 min were adopted as the optimal incubation time for subsequent study.

3.6. The ECL characterization of the amplified strategy

In order to confirm the amplification effect of AuNRs and L-Cys, three kinds of Ab_2 functionalized probes were prepared and the results are shown in Fig. 7 (the green line showed the ECL of BSA/anti-cTnI/GNDs/GCE, the red line showed the ECL of the immunosensor which was incubated with 0.005 ng/mL cTnI and different Ab_2 functionalized probes solution). The Ab_2 functionalized probes are: (*a*) Ab_2/AuNRs/$Ru(dcbpy)_3^{2+}$, (*b*) Ab_2/nano-Au/

L-Cys@Ru(dcbpy)$_3^{2+}$, and (*c*) Ab$_2$/AuNRs/L-Cys@Ru(dcbpy)$_3^{2+}$ (proposed probe).

As illustrated in Fig. 7A, the ECL signal of the immunosensor with the probe of Ab$_2$/AuNRs/Ru(dcbpy)$_3^{2+}$ was 137 a.u. Then the higher emission (about 332 a.u) was produced by adding L-Cys (1 mM) into the working soulation, which demonstrated that L-Cys could act as an proper co-reactant of Ru(dcbpy)$_3^{2+}$. Subequently, AuNRs in the proposed probe was replaced by Au nanoparticles (Nano-Au) to construct the probe *b* (Ab$_2$/Nano-Au/L-Cys@Ru(dcbpy)$_3^{2+}$). The ECL responses of the immunosensor with the probe *b* was 751 a.u. When the immunosensor was incubated with the proposed probe of Ab$_2$/AuNRs/L-Cys@Ru(dcbpy)$_3^{2+}$, the ECL emission raised about 2633 a.u (Fig. 7C). The dramatically enhancement was attributed to three aspects: (1) L-Cys as linking reagent significantly increasing the loading amount of Ru(dcbpy)$_3^{2+}$, (2) AuNRs as carriers could absorb more amount of Ru(dcbpy)$_3^{2+}$, (3) the higher luminous efficiency of L-Cys@Ru(dcbpy)$_3^{2+}$ by the intramolecular ECL reaction. The results adequately indicated that the proposed probes of Ab$_2$/AuNRs/L-Cys@Ru(dcbpy)$_3^{2+}$ could be

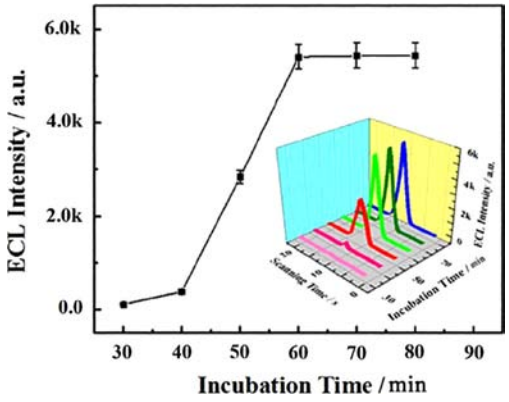

Fig. 6. Optimization of incubation time for Ab$_2$ bioconjugates.

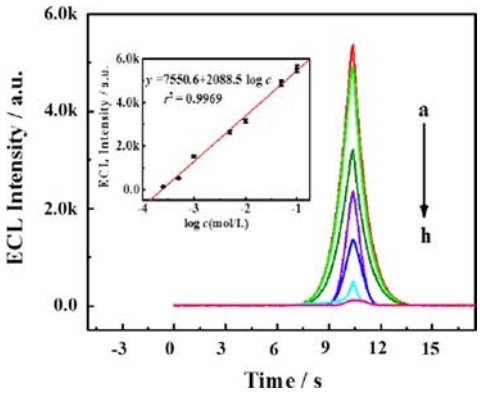

Fig. 8. ECL profiles of the immunosensor in the presence of different concentrations of cTnI based on sandwich-type format in PBS (pH 7.4, 3.0 mL) containing 0.1 M KCl (a)–(h).The concentrations of cTnI: (a) 0.1 ng/mL, (b) 0.05 ng/mL, (c) 0.01 ng/mL, (d) 0.005 ng/mL, (e) 1 pg/mL, (f) 0.5 pg/mL, (h) 0.25 pg/mL.

Table 1
Comparison of our research with other methods for cTnI detection.

Measurement protocol	Linear range/ pg/mL	Detection limit/pg/mL	References
Electrochemical immunoassay	800–5,000	500	Guo et al. [6]
Optomagnetic biosensor	30–6,500	30	Dittmer et al. [5]
ELISA	100–10,000	27	Cho et al. [4]
Electrochemiluminescence	2.5–10,000	2	Shen et al. [26]
Electrochemiluminescence	0.25–100	0.083	Present work

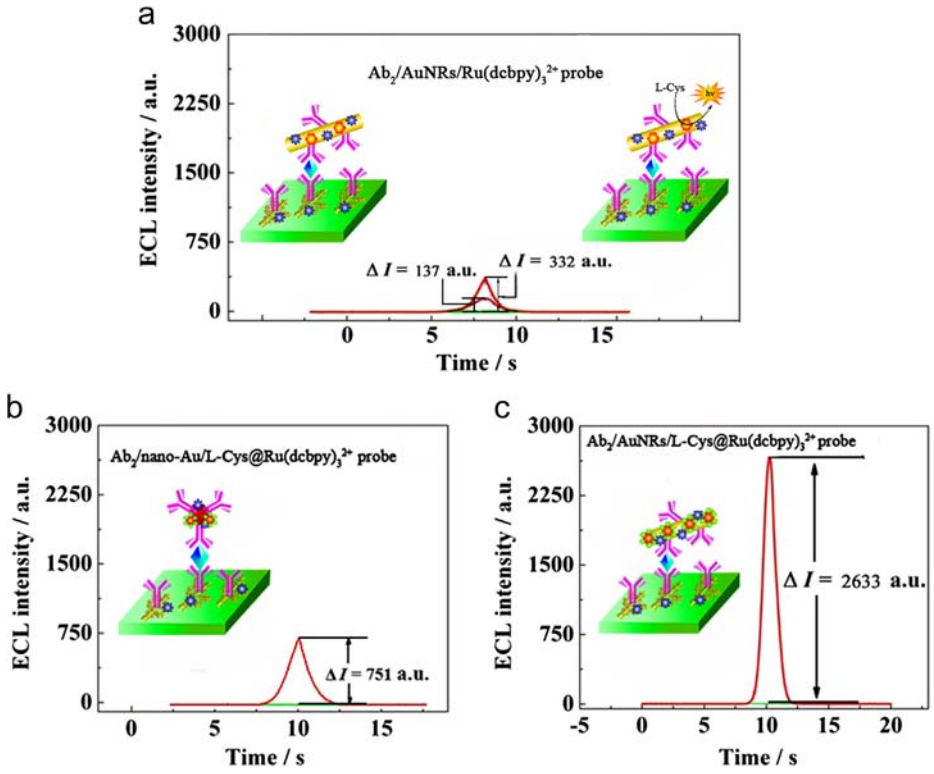

Fig. 7. ECL profiles of the different sandwich format immunosensors in the absence (a, green line) and in the presence of Ab$_2$ bioconjugates (b, red line), by using various labels: (A) Ab$_2$/AuNRs/Ru(dcbpy)$_3^{2+}$ labeled immunosensor, (B) Ab$_2$/nano-Au/L-Cys@Ru(dcbpy)$_3^{2+}$ labeled immunosensor, and (C) Ab$_2$/AuNRs/L-Cys@Ru(dcbpy)$_3^{2+}$ labeled immunosensor. The concentration of cTnI was 0.005 ng/mL. Working solution, PBS (pH 7.4) or PBS (pH 7.4) containing L-Cys (1 mM). Scan rate was 100 mV/s. (For interpretation of the references to color in this figure legend, the reader is referred to the web version of this article.)

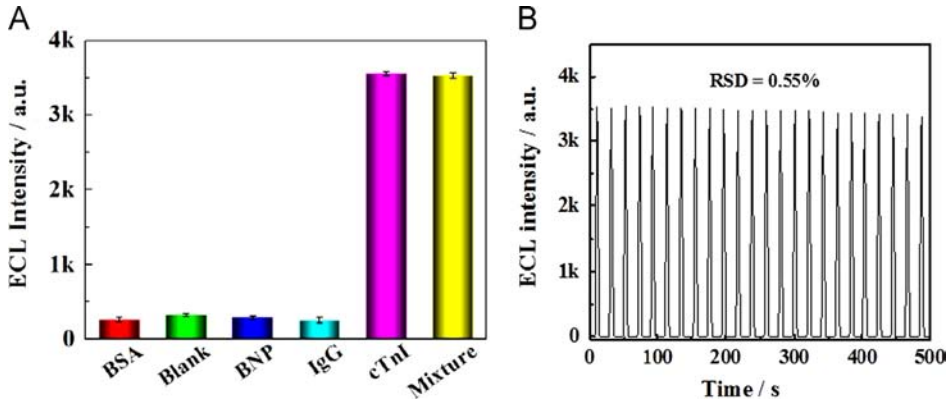

Fig. 9. (A) The selectivity of the proposed ECL immunosensors toward different targets (a) Blank, (b) BSA (0.1 ng/mL), (c) BNP (0.1 ng/mL), (d) IgG (0.1 ng/mL), (e) cTnI (0.01 ng/mL) and (f) a mixture containing BSA (0.1 ng/mL), IgG (0.1 ng/mL), BNP (0.1 ng/mL) and cTnI (0.01 ng/mL). (B) Stability of the proposed ECL immunosensor incubated with 0.01 ng/mL cTnI based on sandwich format under consecutive cyclic potential scans for 24 cycles in PBS (pH 7.4) containing 0.1 M KCl. Scan rate, 100 mV/s.

effectively utilized for ultrasensitive detection of cTnI with the amplification of the ECL signal.

3.7. Analytical performance of ECL immunosensors

Under the optimized experimental conditions, we explored the quantitative range of the proposed ECL immunosensor (Fig. 8). As expected, the ECL intensity increased linearly with the cTnI concentrations in the range from 0.25 pg/mL to 0.1 ng/mL with a detection limit of 0.083 pg/mL ($S/N=3$). The linear regression equation was $y=7550.6+2088.5 \log c$, and the correlation coefficient of $r^2=0.9969$. According to the linear equation, the proposed method could be used to detect cTnI concentration quantitatively. Additionally, we also made a comparative study between proposed immunosensors with previous reported (Table 1) [4,5,25,26], and the proposed immunosensor exhibited more excellent analytical properties for the detection of cTnI compared with reported ECL immunoassay. It is reported that patients with high likelihood of cardiac contusion had cTnI concentrations greater than 2.0 ng/mL [27]. So we can further reduce the interference of other proteins by diluting the serum in the clinical diagnosis, and thus provided a highly efficient and reliable analytical method for measuring cTnI at ultralow levels.

3.8. Stability, reproducibility and selectivity

To investigate the selectivity and specificity of the proposed immunosensor, contrast experiments were performed (see Fig. 9A). Intravenous gamma globulin (IgG), amino-terminal pro-brain natriuretic peptide (BNP) and bovine serum albumin (BSA) were used as interfering substances to evaluate the selectivity. The immunosensors were incubated with 0.1 ng/mL IgG, 0.1 ng/mL BNP and 0.1 ng/mL BSA, respectively. Almost no signal change was obtained compared with the background. The immunosensor was also incubated with 0.01 ng/mL cTnI containing different interfering species, compared with the ECL response obtained from the 0.01 ng/mL cTnI only, no significant difference was found. All these results indicated a good selectivity of the proposed immunosensor.

The stability of proposed immunosensor was investigated by consecutive cyclic potential scans for 24 cycles. As shown in Fig. 9B, the ECL intensity did not show any obvious changes. The outstanding stability may be attributed to AuNRs/L-Cys@Ru $(dcbpy)_3^{2+}$ is a good matrix for the loading of Ab_2, which could increase the access chance of the antigen and antibody.

Simultaneously, the reproducibility of the proposed immunosensor was evaluated by the relative standard deviation (ECL response) of intra- and inter-assays. The relative standard deviations (R.S.D.) of the intra- and inter-assay were not more than 5%. Thus, the reproducibility of the proposed immunoassay was acceptable.

Table 2
Preliminary analysis of real samples.

Sample number	Added/ng/mL	Found/ng/mL	Recovery (%)
1	0.050	0.0520	104
2	0.040	0.0390	97.5
3	0.030	0.0315	105
4	0.025	0.0243	97.2
5	0.010	0.0107	107
6	0.0050	0.00456	91.2

3.9. Preliminary analysis of real samples

Moreover, the practical applicability of the immunosensor has also been investigated using the standard addition method in human blood serum. The results were shown in Table 2 and the recovery and relative standard deviation values were ranging from 91.2% to 107%, which confirmed that the proposed immunosensor could be reasonably applied in the clinical determination of cTnI.

4. Conclusions

In conclusion, we have successfully developed a reagentless ECL immunosensor for the sensitive and specific detection of cTnI based on the self-enhanced electrochemiluminescent L-Cys@Ru $(dcbpy)_3^{2+}$ which combined the coreactant and the luminophor in one molecule. The proposed method avoided the adding of any coreactant into testing solution for signal amplification and thus simplified the operation. Meanwhile, since the intramolecular ECL reaction has the shorter electron transfer path and less energy loss, the proposed immunosensor exhibited more excellent analytical properties for the detection of cTnI and the liner range was from 0.25 pg/mL to 0.1 ng/mL, down one order of magnitude compared with reported ECL immunoassay. Furthermore, it is expected to provide a promising approach for the detection of a wide range of molecular analytes.

Acknowledgments

This work was financially supported by the NNSF of China (21075100, 21275119, 21105081), Ministry of Education of China (Project 708073), Research Fund for the Doctoral Program of

Higher Education (RFDP) (20110182120010), Natural Science Foundation of Chongqing City (CSTC-2011BA7003, CSTC-2010BB4121), State Key Laboratory of Silkworm Genome Biology (sklsgb2013012) and the Fundamental Research Funds for the Central Universities (XDJK2013A008, XDJK2013A27), China.

References

[1] C.J. Murray, A.D. Lopez., Lancet 349 (1997) 1498–1504.
[2] I.K. Tuteja, V. Priyanka, A. Bhalla, A.K. Deep, C.R. Suri. Paulb, Anal. Chim. Acta 232977 (2013) 7.
[3] A. Periyakaruppan, R.P. Gandhiraman, M Meyyappan, J.E. Koehne., Anal. Chem. 85 (2013) 3858–3863.
[4] I.H. Cho, E.H. Paek, Y.K. Kim, J.H. Kim, S.H. Paek., Anal. Chim. Acta 632 (2009) 247–255.
[5] W.U. Dittmer, T.H. Evers, W.M. Hardeman, W. Huijnen, R. Kamps, P. Kievit., Clin. Chim. Acta 411 (2010) 868–873.
[6] H.S. Guo, N.Y. He, S.X. Ge, D. Yang, J. Zhang., Talanta 68 (2005) 61–66.
[7] W.L. Guo, E.Z. Li, H.D. Wang, Adv. Mater. Res. 662 (2013) 68–71.
[8] C.C. Cheng, Y. Huang, X.Q. Tian, B.Z. Zheng, Y. Li, H.Y. Yuan, D. Xiao, S.P. Xie, M.M.F. Choi., Anal. Chem. 84 (2012) 4754–4759.
[9] C.A. Kent, D. Liu, A. Ito, T. Zhang, M.K. Brennaman, T.J. Meyer, W. Lin., J. Mater. Chem. A 1 (2013) 14982–14989.
[10] B.N. Wu, C.Y. Hu, X.Q. Hu, H.M. Cao, C. Huang, H.B. Shen., Biosens. Bioelectron. 50 (2013) 300–304.
[11] H. Dai, Y.M. Wang, X.P. Wu, L. Zhang, G.N. Chen., Biosens. Bioelectron. 24 (2009) 1230–1234.
[12] H.N. Choi, J.Y. Lee, Y.K. Lyu, W.Y. Lee, Anal. Chim. Acta 565 (2006) 48–55.
[13] N. Liao, Y. Zhuo, Y.Q. Chai, Y. Xiang, J. Han, R. Yuan., Biosens. Bioelectron. 45 (2013) 189–194.
[14] K.N. Swanick, S. Ladouceur, E.Z. Colman, Z.F. Ding., Angew. Chem. Int. Ed. 51 (2012) 11079–11082.
[15] M.C. Daniel, D. Astruc., Chem. Rev. 104 (2004) 293–346.
[16] Y.R. Liu, R. Hu, T. Liu, X.B. Zhang, W.H. Tan, G.L. Shen, R.Q. Yu., Talanta 107 (2013) 402–407.
[17] K.S. Lee, M.A. ElSayed., J. Phys. Chem. B 110 (2006) 19220–19225.
[18] B. Nikoobakht, M.A. Elsayed., Chem. Mater. 15 (2003) 1957–1962.
[19] H.X. He, J. Du, Y.Q. Hu, J. Ru, X.Q. Lu., Talanta 115 (2013) 381–385.
[20] J.J. Feng, A.Q. Li, Z. Lei, A.J. Wang., J Am. Chem. Soc. 4 (2012) 2570–2576.
[21] W. Tang, D.B. Chase, J.F. Rabolt., Anal. Chem. 79 (2013) 8584–8589.
[22] H. Herberhold, S. Marchal, R. Lange, C.H. Scheyhing, R.F. Vogel, R. Winter., J. Mol. Biol. 330 (2003) 1153–1164.
[23] S.H. Choi, K.P. Lee, J.G. Lee., Microchem. J. 68 (2001) 205–213.
[24] W.J. Miao, J.P. Choi, A.J. Bard., J. Am. Chem. Soc. 124 (2002) 14478–14485.
[25] F. Torabi, H.R.M. Far, B. Danielsson, M. Khayyami., Biosens. Bioelectron. 22 (2007) 1218–1223.
[26] W. Shen, D.Y. Tian, H. Cui, D. Yang, Z.P. Bian., Biosens. Bioelectron 27 (2011) 18–24.
[27] R. Hirsch, Y. Landt, S. Porter, C.E. Canter, A.S. Jaffe, J.H. Ladenson, J. Pediatr. 130 (1997) 6.